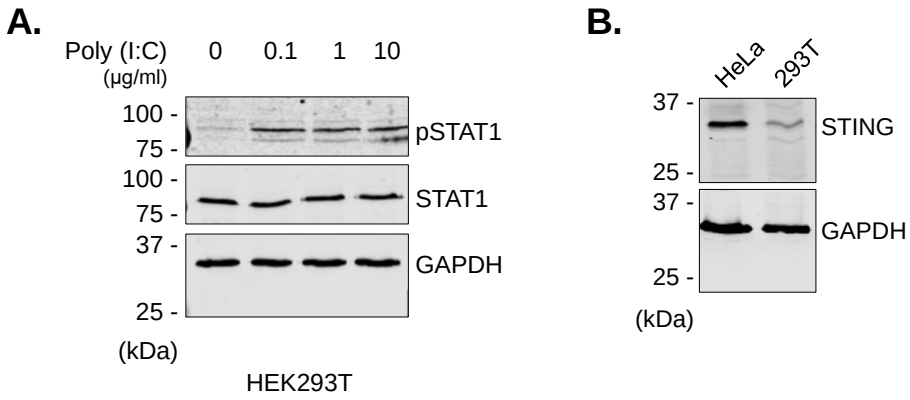

Figure S1. Response to poly (I:C) transfection in HEK293T cells is intact despite lack of STING, Related to Figure 1

(a) HEK293T-CD300lf cells were transfected with indicated amounts of poly(I:C). The cells were harvested 6h after transfection and assessed by western blotting for the indicated proteins.

(b) Lysates from HeLa-CD300lf and HEK293T-CD300lf cells were assessed by western blotting for STING and GAPDH.

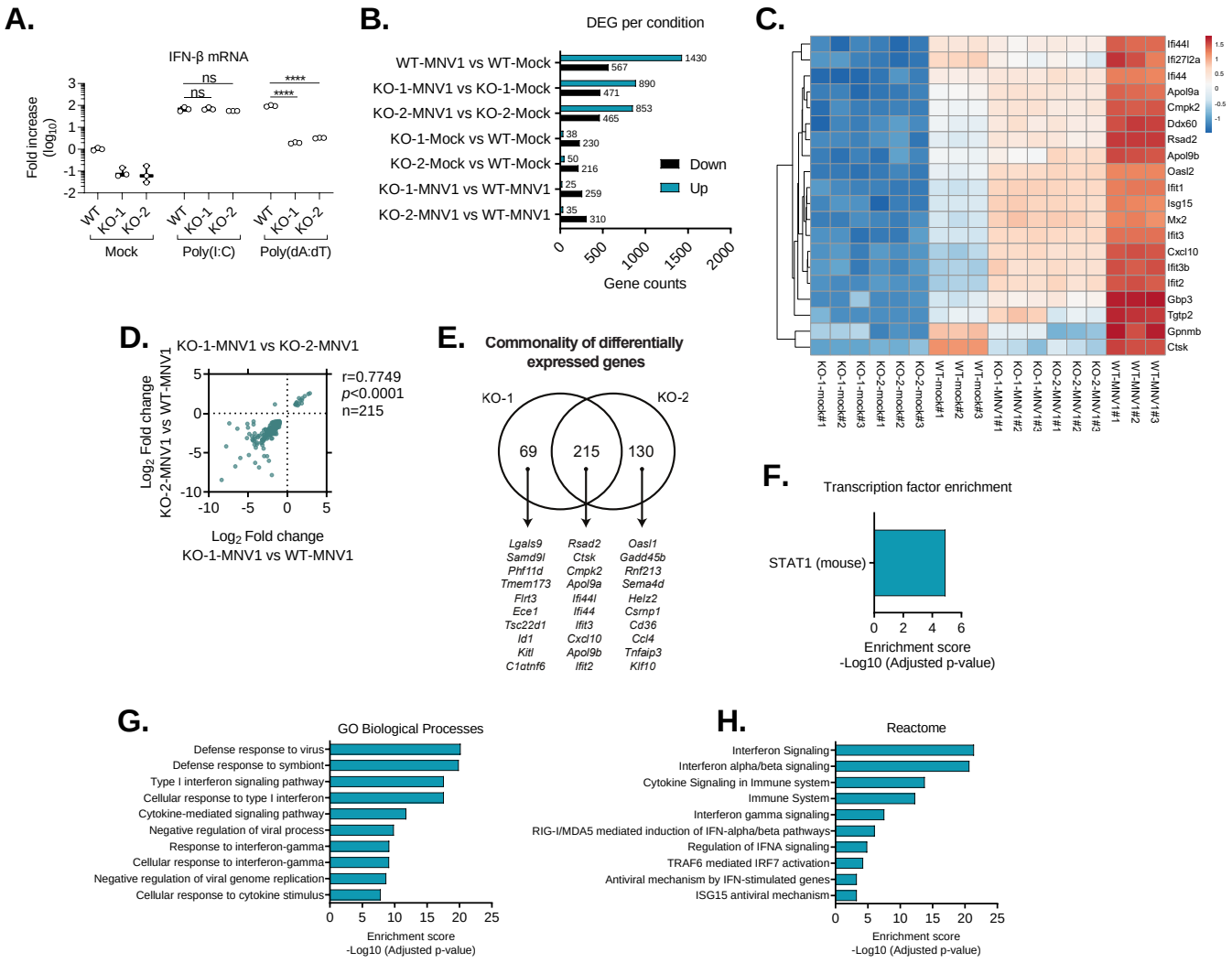

Figure S2. STING knockout impairs IFN induction in MNV-infected cells, Related to Figure 2

(a) STING$^{+/+}$ (WT) and clones 14 and 22 STING$^{-/-}$ (KO-1 and KO-2, respectively) RAW264.7 cells, were mock transfected, transfected with 1µg/ml of Poly(I:C), or with 1µg/ml of Poly(dA:dT) for 6h, and were subsequently harvested and assessed for IFN-β mRNA using RT-qPCR. Data is expressed relative to control and normalised to *Gapdh*.

(b) to (h) STING+/+ (WT) and clones 14 and 22 STING-/- (KO-1 and KO-2, respectively) RAW264.7 cells, were mock infected or infected with wild-type MNV1 at an MOI of 5 and harvested at 9h post-infection. Samples were assessed by total RNA sequencing. (b) Bar chart summarizing total differential gene expression count per condition. (c) Heat map displaying the top 20 differentially expressed genes. (d) Fold change correlation analysis of commonly differentially expressed genes between the indicated comparisons. (e) Venn diagram showing commonality of differentially expressed genes when MNV1-infected KO-1 or KO-2 cells were compared to infected wild-type cells. (f) Transcription factor enrichment analysis on genes from (d). (g) and (h) Gene ontology enrichment (g) and Reactome pathways analysis (h) of genes from (d). Data in (b) to (h) represent a single experiment done in triplicate.

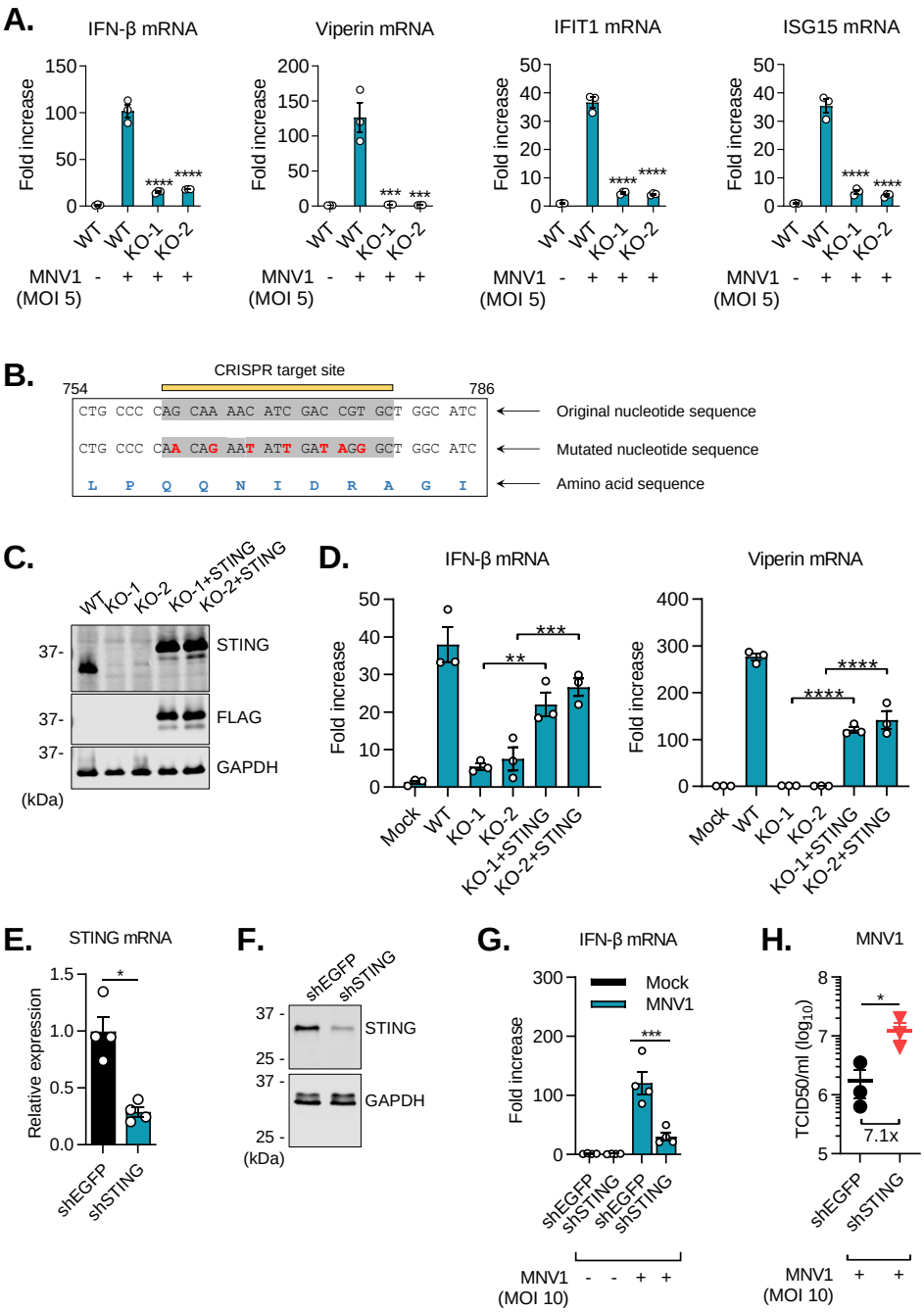

Figure S3. STING is required for a robust IFN response in MNV-infected cells, Related to Figure 2

(a) STING$^{+/+}$ (WT) and clones 14 and 22 STING$^{-/-}$ (KO-1 and KO-2, respectively) RAW264.7 cells, were mock infected or infected with wild-type MNV1 at an MOI of 5 and harvested at 9h post-infection. Samples were assessed for IFN-β mRNA via RT-qPCR. Data is representative of two independent experiments done in triplicates, and is shown relative to mock-infected cells, and normalised to mouse *Gapdh*.

(b) Schematic representation of the silent mutations (red) introduced at the CRISPR target site of STING (shaded grey) prior to complementation in STING KO-1 and KO-2 cells

(c) STING$^{+/+}$ (WT), clones 14 and 22 STING$^{-/-}$ (KO-1 and KO-2, respectively), and STING KO-1 and KO-2 RAW264.7 cells complemented with flag-tagged CRISPR-resistant STING were assessed by western blotting for the indicated proteins.

(d RAW264.7 cells from (c) were mock infected or infected with wild-type MNV1 at an MOI of 5 and harvested at 9h post-infection. Samples were assessed for IFN-β mRNA via RT-qPCR. Data is representative of two independent experiments done in triplicates, and is shown relative to mock-infected cells, and normalised to mouse *Gapdh*.

(e) and (f) RAW264.7 cells stably transduced with control shRNA (shEGFP) or shRNA targeting mouse STING (shSTING-3) were lysed and assessed for STING mRNA via RT-qPCR (e) or analysed via western blotting (f). Data in (e) is presented relative to control and normalised to *Gapdh*.

(g) and (h) RAW264.7 cells stably transduced with control shRNA (shEGFP) or shRNA targeting mouse STING (shSTING-3), were mock infected or infected with wild-type MNV1 at an MOI of 10 and harvested at 9h post-infection. Samples were assessed for IFN-β mRNA via RT-qPCR (c), or infectious viral titres were determined using TCID50 (g). Data in (h) is presented relative to control and normalised to *Gapdh*.

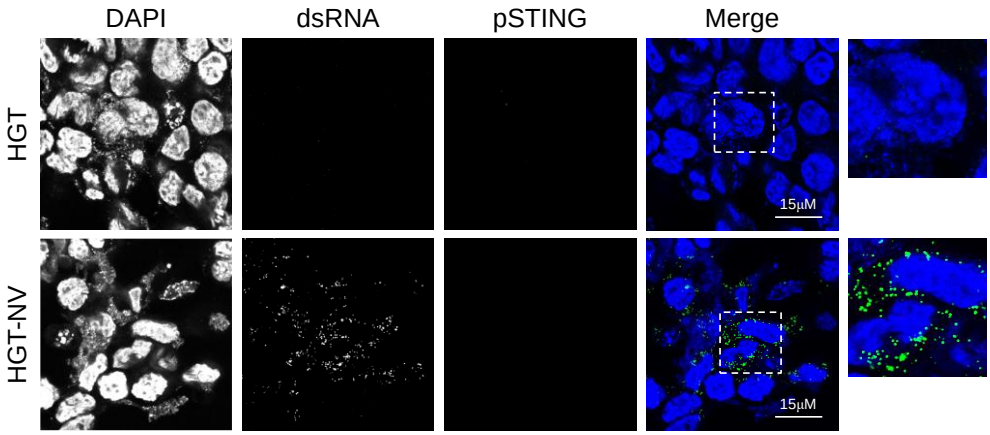

Figure S4. HGT-NV cells do not show evidence of STING phosphorylation, Related to Figure 3

HGT and HGT-NV cells were seeded on coverslips overnight. The cells were then fixed, permeabilised, and stained for pSTING (red), dsRNA (green), and nuclei (blue), and images were acquired using a confocal microscope.

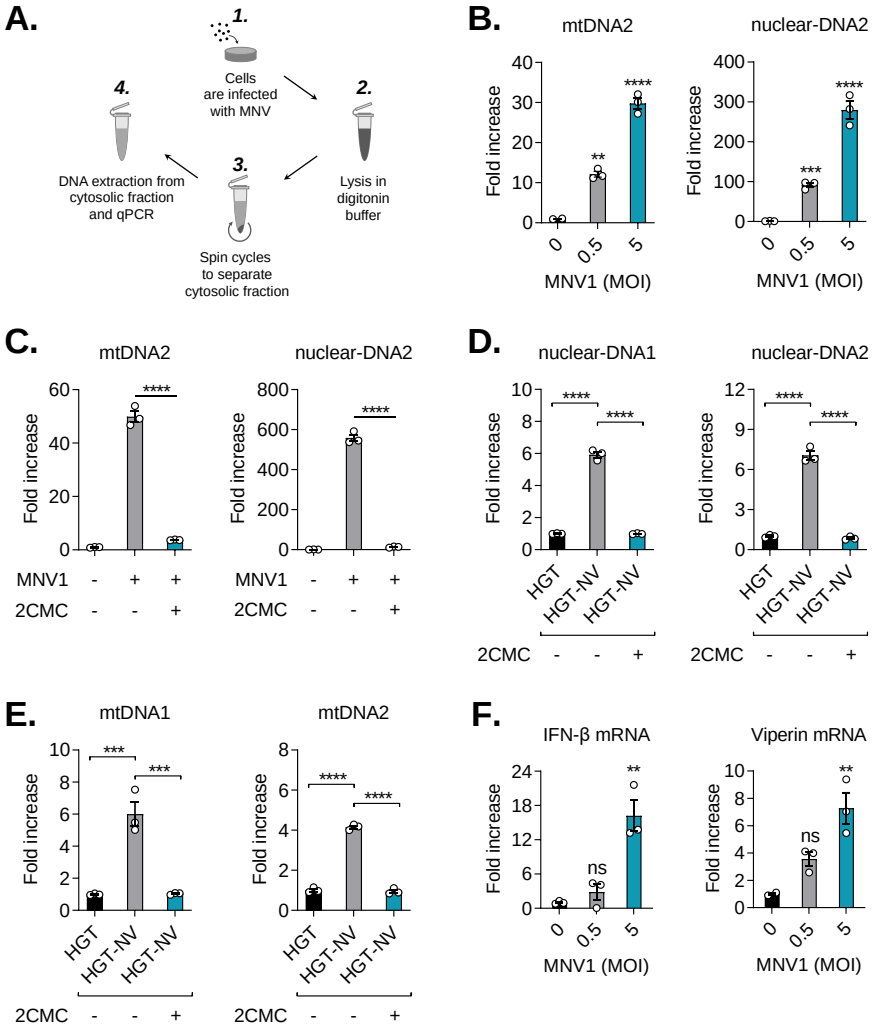

Figure S5. DNA accumulate in the cytosol of norovirus-infected cells, and induces an IFN response, Related to Figure 5

(a) Schematic representation of the cell fractionation and cytosolic DNA extraction protocol.

(b) RAW264.7 cells were either mock-infected or infected with MNV1 at the indicated MOI. The cells were harvested 12h post-infection and assessed for cytosolic DNA by qPCR. Data is representative of two independent experiments done in triplicates, and is shown relative to control and normalised to the whole cell fractions.

(c) RAW264.7 cells were pre-treated with 200 μM 2'-C-methylcytidine (2CMC) for 30 minutes and then infected with MNV1 at an MOI of 5. The cells were harvested 12h post-infection and assessed for cytosolic DNA by qPCR. Data is representative of two independent experiments done in triplicates, and is shown relative to control and normalised to the whole cell fractions.

(d) and (e) HGT and HGT-NV cells were either untreated or treated with 50 μM 2CMC, as indicated. Cells were harvested 72 hours later and assessed for cytosolic DNA by qPCR. Data is representative of two independent experiments done in triplicates, and is shown relative to the untreated HGT control and normalised to the whole cell fractions.

(f) RAW264.7 cells were infected with MNV1 at the indicated MOIs. The cells were harvested and fractionated 12h post-infection, and DNA was extracted from the cytosolic and whole cell fractions. Pre-seeded cells were transfected with normalised amounts of the cytosolic DNA, harvested 9h post transfection, and analysed by qPCR. Data is presented relative to control and normalised to *Gapdh*.

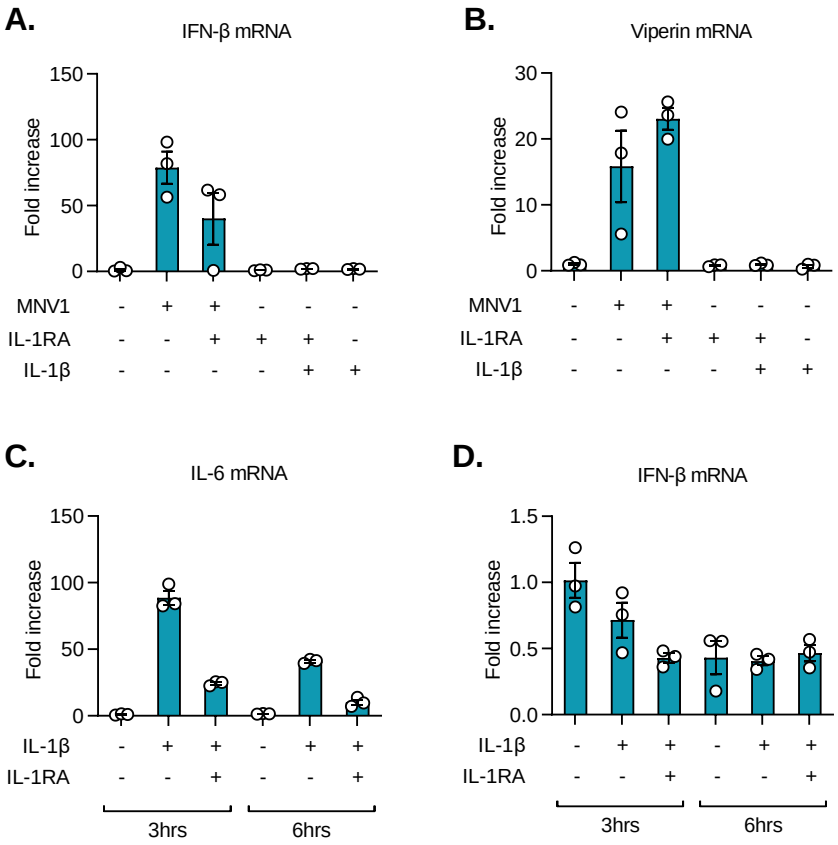

Figure S6. Inhibition of IL-1β signalling did not inhibit IFN responses in MNV-infected RAW264.7 cells, and IL-1β treatment failed to induce IFN-β in A549 cells, Related to Figure 6

(a) and (b) RAW264.7 cells were either mock-treated or treated with 100ng/ml of recombinant IL-1RA for 30 minutes before infection with MNV1 at an MOI of 5, or treatment with 10ng of recombinant mouse IL-1β. The cells were harvested at 12h post-infection and analysed by RT-qPCR. Data is presented relative to control and normalised to *Gapdh*

(c) and (d) A549 cells were either mock-treated or treated with 100ng/ml of recombinant IL-1RA for 30 minutes before treatment with 10ng of recombinant human IL-1β. The cells were harvested at the indicated timepoints and analysed by RT-qPCR. Data is presented relative to control and normalised to β-actin.

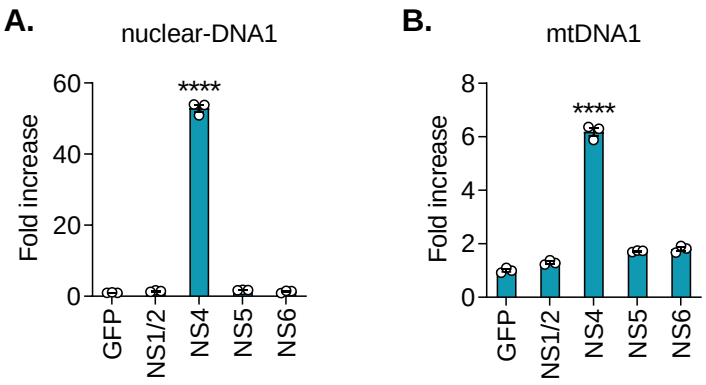

Figure S7. NS4, but not NS1-2, NS5 (VPg) or NS6, is sufficient for leakage of genomic and mitochondrial DNA in cell lines, Related to Figure 6

(a) and (b) HEK293T-CD300lf cells were transfected with Flag-tagged construct plasmids of the indicated proteins. The cells were harvested 24h post transfection and assessed for cytosolic DNA by qPCR. Data is presented relative to GFP and normalised to their corresponding whole cell fractions.

Table S1: List of plasmids used, Related to STAR Methods

sn	**Name**	**Insert/description**	**Source**	**Comments**
1.	pT7:MNV-1_3'Rz	MNV1 WT cDNA clone	Chaudhry *et al.* 2007[S1]	For generating wild-type MNV1
2.	pT7:MNV-1_3'Rz_M1	MNV1 M1 cDNA clone	McFadden *et al.* 2011[S2]	Similar to pT7:MNV-1_3'Rz, but with a T5118A mutation that introduces a stop codon 17 amino acids downstream of the VF1 start codon and a silent mutation in VP1
3.	pFS669IG	Mouse CD300lf	This work	
4.	pMDLg/pRRE	Encodes Gag and Pol; contains the rev response element	Dull *et al.* 1998[S3]	3rd generation lentiviral packaging plasmid, Addgene #12251
5.	pRSV-Rev	Encodes Rev	Dull *et al.*1998[S3]	3rd generation lentiviral packaging plasmid, Addgene #12253
6.	pMD2G	VSV-G envelop plasmid	Dull *et al.*1998[S3]	3rd generation lentiviral packaging plasmid, Addgene #12259
7.	shEGFP	shRNA sequence targeting EGFP	Sigma (SHC005)	MISSION pLKO.1-puro Control Plasmid
8.	shSTING-3	Mouse STING (TMEM173) shRNA	Sigma (SHCLNG-NM_028261)	MISSION shRNA plasmid TRCN0000346266
9.	pAJ093IG	FLAG-EGFP	This work	Gateway cloning; N-terminal tag
10.	pFS610IG	FLAG-NS1-2	This work	MNV1 protein, Gateway cloning, N-terminal tag
11.	pFS611IG	FLAG-NS3	This work	MNV1 protein, Gateway cloning, N-terminal tag
12.	pFS612IG	FLAG-NS4	This work	MNV1 protein, Gateway cloning, N-terminal tag
13.	pFS613IG	FLAG-NS5	This work	MNV1 protein, Gateway cloning, N-terminal tag
14.	pFS614IG	FLAG-NS6	This work	MNV1 protein, Gateway cloning, N-terminal tag
15.	pFS615IG	FLAG-NS7	This work	MNV1 protein, Gateway cloning, N-terminal tag
16.	pFS616IG	FLAG-VF1	This work	MNV1 protein, Gateway cloning, codon-optimised, N-terminal tag
17.	pFS621IG	FLAG-VP1	This work	MNV1 protein, Gateway cloning, N-terminal tag
18.	pFS617IG	FLAG-VP2	This work	MNV1 protein, Gateway cloning, N-terminal tag
19.	pAJ124IG	FLAG-GII.4-NS4	This work	HuNoV protein, Gateway cloning, N-terminal tag

20.	pAJ221IG	mouse STING sgRNA	This work	sgRNA sequence AGCAAAACATCGACCGTGC (previously reported by Storek *et al*.[S4]), cloned into LentiCRISPRv2 (Addgene #52961[S5])
21.	pAJ222IG	FLAG-tagged CRISPR-resistant mouse STING	This work	Overlap-extension PCR and digestion ligation cloning

Table S2: List of antibodies used, Related to STAR Methods

sn	**Target**	**Purpose**	**Supplier**	**Catalogue Number**	**Dilution**
1.	Mouse GAPDH	Western blot	Ambion	AM4300	1:20000
2.	Human GAPDH	Western blot	Protein Tech	10494-1-AP	1:20000
3.	Human IRF3	Western blot	Abclonal	A11373	1:250
4.	Human pIRF3	Western blot	Abcam	ab138449	1:500
5.	STAT1	Western blot	Abcam	ab92506	1:500
6.	pSTAT1	Western blot	Cell signalling	9167S	1:500
7.	STING (D2P2F)	Western blot	Cell signalling	13647	1:500
8.	NS3	Western blot	Non-commercial	-	1:500
9.	VPg	Western blot	Non-commercial	-	1:500
10.	NS7	Western blot	Non-commercial	-	1:500
11.	pSTING (Ser366, clone E9A9K) (rabbit)	Confocal (1^{o})	Cell signalling	50907S	1:1500
12.	dsRNA (J2) (mouse)	Confocal (1^{o})	Cell signalling	76651	1:1000
13.	Alexa-flour 488 goat anti-mouse IgG (H+L)	Confocal (2^{o})	Invitrogen	A-11029	1:1000
14.	Alexa-flour 568 goat anti-rabbit IgG (H+L)	Confocal (2^{o})	Invitrogen	A-11011	1:1000

Table S3: List of RT-qPCR Primers used, Related to STAR Methods

sn	**Target**	**Lab no.**	**Sequence (FWD, REV)**	**Ref.**
1.	Mouse *Ifnb1* (IFN- β)	IGUC0339 IGUC0340	ATGAACAACAGGTGGATCCTCC AGGAGCTCCTGACATTTCCGAA	Petro 2005[S6]
2.	Mouse *Rsad2* (Viperin)	IGUC1898 IGUC1899	GGTTCAAGGACTATGGGGAGTATTTGGAC GAAATCTTTCTGCTTCCCTCAGGGCATC	This work
3.	Mouse *Ifit1*	IGUC1052 IGUC1053	CTGAGATGTCACTTCACATGGAA GTGCATCCCCAATGGGTTCT	This work
4.	Mouse *Isg15*	IGUC1902 IGUC1903	GGTAACGATTTCCTGGTGTCCG GCTCAGCCAGAACTGGTCTTCG	This work
5.	Mouse *Gapdh*	IGUC0945 IGUC0946	CATGGCCTTCCGTGTTCCTA GCGGCACGTCAGATCCA	Wu et al. 2008[S7]
6.	Human *ACTB* (β-actin)	IGUC0784 IGUC0785	TTCTACAATGAGCTGCGTGTG GGGGTGTTGAAGGTCTCAAA	Egerod et al. 2007[S8]
7.	Human *IFNB1* (IFN- β)	IGUC0772 IGUC0773	CAGAAGGAGGACGCCGCATTGAC CCAGGCACAGTGACTGTACTCC	Hooks et al. 2008[S9]
8.	Human *RSAD2* (Viperin)	IGUC2411 IGUC2412	CCTGTCCGCTGGAAAGTGTT GACACTTCTTTGTGGCGCTC	This work
9.	Human *IL6* (IL-6)	IGUC1231 IGUC1232	ACTCACCTCTTCAGAACGAATTG CCATCTTTGGAAGGTTCAGGTTG	Di Lorenzo et al. 2014[S10]

Table S4: List of genomic and mtDNA qPCR Primers used, Related to STAR Methods

sn	**Target**	**Lab no.**	**Sequence (FWD, REV)**	**Ref.**
1.	Mouse nuclear-DNA1 (*Gapdh*)	IGUC4428 IGUC4429	CGTTGAATTTGCCGTGAGTG CACTACAGACCCATGAGGAGT	This work
2.	Mouse nuclear-DNA2 (*Hprt*)	IGUC4432 IGUC4433	CCACTTGTGACGAAAGCACC GTTGTCTACGCTCTGGCAGT	This work
3.	Mouse mtDNA1 (*Cox1*)	IGUC4405 IGUC4406	TCGGAGCCCCAGATATAGCATT CTGCTCCTGCTTCTACTATTGATG	Ma *et al.* [S11]
4.	Mouse mtDNA2 (*Cox1*)	IGUC4219 IGUC4220	GCCCCAGATATAGCATTCCC GTTCATCCTGTTCCTGCTCC	Moriyama *et al.* [S12]
5.	Human nuclear-DNA1 (*18S*)	IGUC4442 IGUC4443	TAGAGGGACAAGTGGCGTTC CGCTGAGCCAGTCAGTGT	Aguirre *et al.*[S13]
6.	Human nuclear-DNA2 (*GAPDH*)	IGUC4440 IGUC4441	CTCTGCTCCTCCTGTTCGAC AATCCGTTGACTCCGACCTT	Aguirre *et al.* [S13]
7.	Human mtDNA1 (*ND1*)	IGUC4444 IGUC4445	CACCCAAGAACAGGGTTTGT TGGCCATGGGTATGTTGTTAA	Aguirre *et al.* [S13]
8.	Human mtDNA2 (D-loop region)	IGUC4446 IGUC4447	CTATCACCCTATTAACCACTCA TTCGCCTGTAATATTGAACGTA	Aguirre *et al.* [S13]

Table S6: STING transcript assessment by RNAseq in STING-KO RAW264.7 cells following CRISPR/Cas9 sgRNA transduction, Related to STAR Methods

Target gene	sgRNA sequence	Cell line	Clone name	Allele	Mutation site	Mutation type
Tmem173 (STING)	AGCAAAACATCGACCGTGC	STING-KO-1	Clone 14	1	A747-A1094	Deletion
				2	G857-G1095	Deletion
				3	G855-A1097	Deletion
		STING-KO-2	Clone 22	1	G1930	Deletion

Supplemental references

S1. Chaudhry, Y., Skinner, M.A., and Goodfellow, I.G. (2007). Recovery of genetically defined murine norovirus in tissue culture by using a fowlpox virus expressing T7 RNA polymerase. J. Gen. Virol. 88, 2091–2100. 10.1099/vir.0.82940-0.

S2. McFadden, N., Bailey, D., Carrara, G., Benson, A., Chaudhry, Y., Shortland, A., Heeney, J., Yarovinsky, F., Simmonds, P., Macdonald, A., et al. (2011). Norovirus regulation of the innate immune response and apoptosis occurs via the product of the alternative open reading frame 4. PLoS Pathog. 7, e1002413. 10.1371/journal.ppat.1002413.

S3. Dull, T., Zufferey, R., Kelly, M., Mandel, R.J., Nguyen, M., Trono, D., and Naldini, L. (1998). A Third-Generation Lentivirus Vector with a Conditional Packaging System. J. Virol. 72, 8463–8471. 10.1128/JVI.72.11.8463-8471.1998.

S4. Storek, K.M., Gertsvolf, N.A., Ohlson, M.B., and Monack, D.M. (2015). cGAS and Ifi204 Cooperate To Produce Type I IFNs in Response to Francisella Infection. J. Immunol. 194, 3236–3245. 10.4049/JIMMUNOL.1402764.

S5. Sanjana, N.E., Shalem, O., and Zhang, F. (2014). Improved vectors and genome-wide libraries for CRISPR screening. Nat. Methods 2014 118 11, 783–784. 10.1038/nmeth.3047.

S6. Petro, T.M. (2005). ERK-MAP-kinases differentially regulate expression of IL-23 p19 compared with p40 and IFN-β in Theiler's virus-infected RAW264.7 cells. Immunol. Lett. 97, 47–53. 10.1016/j.imlet.2004.09.013.

S7. Wu, Y., Li, Y.-Y., Matsushima, K., Baba, T., and Mukaida, N. (2008). CCL3-CCR5 axis regulates intratumoral accumulation of leukocytes and fibroblasts and promotes angiogenesis in murine lung metastasis process. J. Immunol. 181, 6384–6393. 10.4049/JIMMUNOL.181.9.6384.

S8. Egerod, K.L., Holst, B., Petersen, P.S., Hansen, J.B., Mulder, J., Hökfelt, T., and Schwartz, T.W. (2007). GPR39 splice variants versus antisense gene LYPD1: expression and regulation in gastrointestinal tract, endocrine pancreas, liver, and white adipose tissue. Mol. Endocrinol. 21, 1685–1698. 10.1210/ME.2007-0055.

S9. Hooks, J.J., Nagineni, C.N., Hooper, L.C., Hayashi, K., and Detrick, B. (2008). IFN-beta provides immuno-protection in the retina by inhibiting ICAM-1 and CXCL9 in retinal pigment epithelial cells. J. Immunol. 180, 3789–3796. 10.4049/JIMMUNOL.180.6.3789.

S10. Di Lorenzo, A., Yang, Y., Macaluso, M., and Bedford, M.T. (2014). A gain-of-function mouse model identifies PRMT6 as a NF-κB coactivator. Nucleic Acids Res. 42, 8297. 10.1093/NAR/GKU530.

S11. Ma, H., Qian, W., Bambouskova, M., Collins, P.L., Porter, S.I., Byrum, A.K., Zhang, R., Artyomov, M., Oltz, E.M., Mosammaparast, N., et al. (2020). Barrier-to-autointegration factor 1 protects against a basal cGAS-STING response. MBio 11. 10.1128/MBIO.00136-20.

S12. Moriyama, M., Koshiba, T., and Ichinohe, T. (2019). Influenza A virus M2 protein triggers mitochondrial DNA-mediated antiviral immune responses. Nat. Commun. 10. 10.1038/S41467-019-12632-5.

S13. Aguirre, S., Luthra, P., Sanchez-Aparicio, M.T., Maestre, A.M., Patel, J., Lamothe, F., Fredericks, A.C., Tripathi, S., Zhu, T., Pintado-Silva, J., et al. (2017). Dengue virus NS2B protein targets cGAS for degradation and prevents mitochondrial DNA sensing during infection. Nat. Microbiol. 2, 17037. 10.1038/nmicrobiol.2017.37.